Qualitative Transitions in Object Reorienting Behaviour, Part 2: The Effects of Varying the Centre of Mass

Graham E. Deacon, Mark Wright, and Chris Malcolm

DAI Research Paper No. 864

To appear in the Proceedings of IEEE/RSJ International Conference on Intelligent Robots and Systems, Grenoble, France, September 1997.

Qualitative Transitions in Object Reorienting Behaviour, Part 2: The Effects of Varying the Centre of Mass.

Graham E. Deacon, Mark Wright[1] and Chris Malcolm

Department of Artificial Intelligence, University of Edinburgh,
5 Forrest Hill, Edinburgh, EH1 2QL, Scotland.

{ged, markwr, cam}@dai.ed.ac.uk

Abstract

In this and a companion paper we investigate the topology of the space of possible pushing behaviour for 2.5D objects of arbitrary outline. We do this by studying the Push-Stability Diagram (PSD) derived by Brost, which is a generalisation of a result of Mason's. In a previous paper we showed how to generalise the PSD to objects of arbitrary outline, and the affect of varying the coefficient of friction on the topology of the PSD. In this paper we show how to predict some of the effects on the topology of the PSD that arise from varying the position of the centre of mass, making it possible to use this as a control parameter in the design of objects for feeding.

1 Introduction

In recent years a number of researchers have studied the sliding behaviour of objects. Much of this work has been precipitated by Mason's Ph.D. [11] where he derived a simple rule to determine the sense of reorientation of an object being pushed on a horizontal surface that is independent of the contact pressure distribution. Peshkin [14] considered all possible contact pressure distributions in order to derive conservative estimates on the rate of reorientation of an object. This, in conjunction with Mason's results, allowed him to deduce sequences of fences to be suspended over a conveyor belt so that objects fed at one end would leave at the other in a known orientation to within an interval of uncertainty. This interval of uncertainty was removed in [2] by curving the ends of the fences appropriately. Brost [3], [4] employed Mason's results in order to generate robust grasping strategies for polygonal objects. Goldberg [9] built on Brost's analysis and developed an algorithm that can generate a sequence of squeezing actions that can reorient a polygon from an initially unknown orientation to a known one (with a 180^o ambiguity) by exploiting a parallel jaw gripper with one jaw that is free to slide laterally. Rao and Goldberg [15] extended this algorithm to apply to parts containing algebraic curves. Recently [16] Goldberg's algorithm has also been adapted to synthesise orienting strategies for polygonal objects on conveyor belts fitted with the curved fences reported in [2]. Brost's [3], [4] analysis included the derivation of the Push-Stability Diagram (PSD), which was exploited in [7] to derive optimal length plans to orient a polygonal object for a given value of friction between pushing and pushed objects. In [8] we show how to extend the PSD to arbitrarily shaped objects and how variation in the coefficient of friction can affect the topology of a PSD and thereby influence the length of pushing plans. In this paper we consider how variation in the position of an object's centre of mass (CoM) affects the topology of a PSD.

[1] Current address: Edinburgh Virtual Environment Centre, James Clerk Maxwell Building, The University of Edinburgh, Mayfield Road, Edinburgh, EH9 3JZ, Scotland. Email: Mark.Wright@ed.ac.uk

2 Background

2.1 Mason's Rule

The result of Mason's that precipitated this work we shall just refer to as Mason's rule. It presupposes a quasi-static model of manipulation where Coulomb's law of dry friction applies. A geometric representation of Coulomb friction is the friction cone [13]. If μ is the coefficient of friction, then the friction cone at a point contact is formed by the set of vectors that make an angle θ with the normal at the point of contact, where $\tan\theta = \mu$. Since we will be considering essentially planar tasks, the friction cone will be represented by its projection onto a plane parallel to the surface of sliding.

Mason's rule can be stated as follows: Let R_l and R_r be the left and right rays delimiting the edges of the friction cone, and R_p the ray denoting the direction of pushing. These rays vote relative to the CoM to determine which way the object will rotate; that is to say, if two or more of these rays lie to the left of the line joining the point of contact to the CoM, then the object will rotate clockwise, if two or more of these rays lie to the right of this line, then the object will rotate anticlockwise. If one ray lies on the line from the point of contact to the CoM, and the other two are distributed one on each side of this line, pure translation occurs.

2.2 The Push-Stability Diagram

Brost's push-stability diagram [3], [4] represents, for a given value of the coefficient of friction between a fence and object, the outcome of a particular pushing operation given the initial orientation of the object, and the direction of pushing[2]. In essence it evaluates Mason's rule for all possible object orientations and pushing directions. To represent this graphically Brost constructs what he calls the *operation space* for the task by plotting pushing direction, δ, against object orientation, ϕ.

In addition to Mason's mechanics assumptions Brost assumes that the length of the pushing fence can be considered to be infinitely long. This simplifies the analysis since the behaviour of objects that possess concavities becomes equivalent to that of their convex hulls.

Brost's original algorithm for constructing a PSD was limited to polygonal shapes. In [8] we show that the PSDs for arbitrarily shaped objects can be constructed in a straightforward manner which we will now describe.

Imagine traversing the object's outline and constructing the tangent at each point on its boundary. This represents the fence making contact at that point. We can also construct the normal at each point, and the friction cone rays would make angles of $\pm\theta$ to it. Finally, if we construct a line from the point of contact to the CoM we have defined the decision boundary about which the rays involved in Mason's rule must vote. We will call this the *vote transition boundary* (VTB) and its orientation is measured with respect to the fence in an anticlockwise sense by the angle ψ. See Figure 1.

If we plot the locus of all the vote transition boundaries on the operation space we arrive at what we call the *vote transition curve* (VTC). The values of ψ thus plotted are the critical values for the pushing ray, *i.e.* to the left of this curve the pushing direction votes anticlockwise, and to its right clockwise, so we will colour to the left black to denote an anticlockwise vote, and to the right grey to denote a clockwise vote. In the absence of friction we would be finished at this point. To include the effects of the friction cone rays we note that they maintain a constant relationship to the pushing fence and plot them as the two lines $\delta = \frac{\pi}{2} \pm \theta$ rads. We denote these values as δ_{rfc} and δ_{lfc} for the right and left friction cone rays respectively. Now, everything on the PSD votes relative to

[2]We ought to mention that the Edge Stability Map of Mani and Wilsons' [10], which was derived independently, is a version of the PSD and can be used to give the same information.

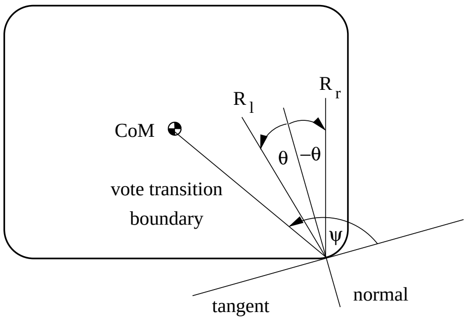

Figure 1: Reorientation sense voting for a curved object.

the VTC, so where δ_{rfc} cuts a lobe of the VTC we draw horizontal lines to the left and colour the bands in between them grey: for all these orientations both friction cone rays lie to the right of the VTC thus determining the sense of the vote as clockwise, regardless of what the pushing ray votes for. Where δ_{lfc} crosses the VTC we draw horizontal lines to the right and colour these bands black for similar reasons. The resulting black regions represent anticlockwise orientation, and the grey clockwise. Examples can be seen in Figures 6 through 9

Note that where an anticlockwise reorienting region (black) lies below a clockwise reorienting region (grey), the boundary between the two regions defines orientations that are stable with respect to the pushing fence, that is to say that for object orientations that lie either side of the boundary, a push in the range of directions for which this boundary is defined, will lead to the object reorienting into this orientation. Consequently, such a boundary is known as a convergent boundary. When the ordering of the regions is reversed the boundary is unstable since on both sides of the boundary, when pushed, the object would reorient away from it. It is these properties that make the PSD useful for feeding purposes [7].

Since the VTC is defined as the locus of the angles between all points on an object's outline and its CoM, and the VTC plays a critical role in the partitioning of the PSD operation space, changing the position of the CoM can obviously change the character of the PSD. This means that there are positions of the CoM that are on the boundary of a change in the topology of the PSD, making the behaviour possible under pushing critically dependent on the CoM's position. We would like to be able to predict these positions because they will affect the robustness of pushing plans, and because the CoM might be used as a control parameter in the design of an object for feeding.

To predict when a change in the position of the CoM results in a change in the topology of the PSD we first note that the decision boundaries partitioning the PSD occur where Mason's rule predicts a rotational equilibrium, *i.e.* translational motion is predicted. These equilibria are either stable or unstable as described above. To predict when qualitative changes in a PSD occur we will perform an analysis of these equilibria. In order to do this we need to introduce some differential geometry.

3 The Frenet-Serret Equations for Planar Curves

Consider a spatial curve $\mathcal{C}$ which is a function of the parameter t. We can write $\mathcal{C}$ as

$$\mathbf{r}(t) = x(t)\mathbf{i} + y(t)\mathbf{j} + z(t)\mathbf{k} \tag{1}$$

where $\mathbf{i}$, $\mathbf{j}$ and $\mathbf{k}$ are unit vectors in the x, y and z directions respectively of some fixed frame of reference, and t lies in some interval of real values. We can let t be arc-length in order to simplify things slightly since in this case (see for example [6], [5])

$$\mathbf{r}'(t) = \mathbf{T}(t) \tag{2}$$

where ' denotes $\frac{d}{dt}$, and $\mathbf{T}(t)$ is the unit tangent vector to $\mathcal{C}$. In this case $\mathcal{C}$ is called a unit speed curve [5].

The basic set of equations for dealing with curves in differential geometry are known as the Frenet-Serret equations (see for example [6], [5]):

$$\begin{aligned}
\mathbf{T}'(t) &= \kappa(t)\mathbf{N}(t) \\
\mathbf{N}'(t) &= -\kappa(t)\mathbf{T}(t) + \tau(t)\mathbf{B}(t) \\
\mathbf{B}'(t) &= -\tau(t)\mathbf{N}(t)
\end{aligned}$$

where $\mathbf{N}(t)$ is the unit normal to the curve, and $\mathbf{B}(t)$ is a unit vector defined by

$$\mathbf{B}(t) = \mathbf{T}(t) \times \mathbf{N}(t) \tag{3}$$

called the binormal. The vectors $\mathbf{T}(t)$, $\mathbf{N}(t)$ and $\mathbf{B}(t)$, in that order, form a right-handed coordinate system. The variable $\kappa(t)$ is the curvature of $\mathcal{C}$, and $\rho(t) = \frac{1}{\kappa(t)}$ is the radius of curvature. The centre of curvature lies a distance $\rho(t)$ along $\mathbf{N}(t)$. The vectors $\mathbf{T}(t)$ and $\mathbf{N}(t)$ define a plane called the osculating plane. The torsion $\tau(t)$ is a measure of the tendency of a curve to twist out of its osculating plane.

Since the curves we are interested in are planar their torsion is zero so the Frenet-Serret equations reduce to the following:

$$\begin{aligned}
\mathbf{T}'(t) &= \kappa(t)\mathbf{N}(t) && (4) \\
\mathbf{N}'(t) &= -\kappa(t)\mathbf{T}(t) && (5) \\
\mathbf{B}'(t) &= \mathbf{0}
\end{aligned}$$

In addition equation (1) reduces to

$$\mathbf{r}(t) = x(t)\mathbf{i} + y(t)\mathbf{j} \tag{6}$$

In what follows we will take $(x(t), y(t))$ of equation (6) to be measured from the CoM of some object that we are interested in, *i.e.* $\mathbf{r}(t)$ is a vector from the centre of mass to a point on the object's perimeter. Also, because t lies on some interval of real values we can consider the curve to come with an orientation: if we consider t increasing the orientation of a closed curve without self crossings is usually chosen such that the interior of the curve lies to the left as the curve is traversed. For the sake of convenience we will omit the arc-length parameter t as an argument in what follows.

4 Conditions for Equilibrium and Stability under Pushing

4.1 When does an equilibrium occur?

To establish the conditions for equilibrium under pushing (*i.e.* when the object is in pure translation without any rotation), it might seem that the most straightforward way to proceed would be to consider a force acting along the inward normal at a contact point. We could then find when the moment generated by this force, with respect to the CoM was equal to zero and thus deduce the conditions for equilibrium. We do not follow this method because the forces on the object may be indeterminate. Instead, we appeal to Mason's rule which circumvents this difficulty (see [11], [12] for a discussion of these issues).

When deciding the outcome of the vote according to Mason's rule the ray that is between the other two is critical since if the sense of reorientation that it votes for changes, then the outcome of the whole vote changes. Consequently, we will refer to the ray which lies between the other two as the *critical ray*.

Consider a typical contact between a fence and a curved object as in Figure 2. Assume the direction of the critical ray is at an angle γ to the contact normal. We will determine the sense of the critical ray's vote by defining the vector cross product $\mathbf{M}_\gamma$ as in Figure 2. To define $\mathbf{M}_\gamma$ we have transformed the critical ray into a vector of unit length, $\mathbf{N}_\gamma$; the length is not important as we are only interested in the *sign* of the product. Using $\times$ to denote vector product, $\mathbf{M}_\gamma$ is given by:

$$\mathbf{M}_\gamma = \mathbf{r} \times \mathbf{N}_\gamma \tag{7}$$

It will be useful to refer to the magnitude of $\mathbf{M}_\gamma$ which we will call M_γ. The relationship between the cross prod-

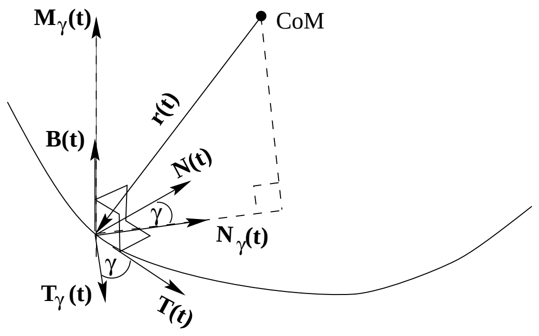

Figure 2: Geometry of a typical contact.

uct $\mathbf{M}_\gamma$ and its magnitude M_γ is given by:

$$\mathbf{M}_\gamma = M_\gamma \mathbf{B}$$

This follows from (3) since $\mathbf{r}$ and $\mathbf{N}_\gamma$ both lie in the osculating plane, hence $\mathbf{M}_\gamma$ is in the direction of $\mathbf{B}$.

The vote of the critical ray is defined by the *sign* of the scalar M_γ. If M_γ is positive then the vote was to the right of the CoM and the rotation is positive, *i.e.* anti-clockwise. Conversely, if M_γ is negative then the vote was to the left of the CoM and the rotation is negative, *i.e.* clockwise.

Using Mason's rule we know that at equilibrium the critical ray passes through the CoM. So in terms of the cross product (assuming the magnitude of the critical ray $\neq 0$)

$$0 = \mathbf{r} \times \mathbf{N}_\gamma$$

i.e. $\mathbf{r}$ is parallel to $\mathbf{N}_\gamma$, and $M_\gamma = 0$.

4.2 When is an equilibrium stable?

We will now determine under what conditions an equilibrium will be stable to perturbation and in what conditions it will be unstable. We can do this by perturbing the object either side of an equilibrium and noting the effect of the critical ray on the behaviour of the object using Mason's rule.

Consider the object contact depicted in Figure 3(b). For ease of explanation we show the critical ray as normal to the point of contact, *i.e.* $\gamma = 0$: no loss of generality results. The contact is at point B and the critical ray extends vertically up from B to pass through the CoM. The object is therefore in equilibrium and the magnitude M_γ of the cross product $\mathbf{M}_\gamma$ is zero.

In Figure 3(a) the object has been perturbed from equilibrium such that the contact point is at point A and the critical ray extends vertically up from A. The critical ray passes to the left of the CoM and thus the

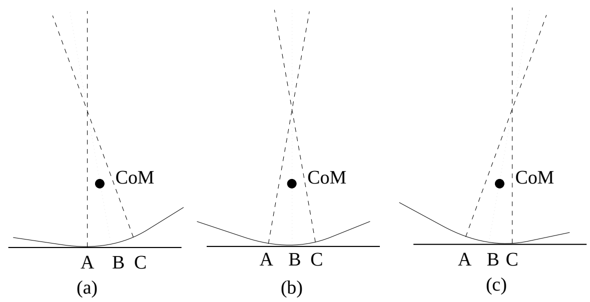

Figure 3: Perturbations about a stable equilibrium.

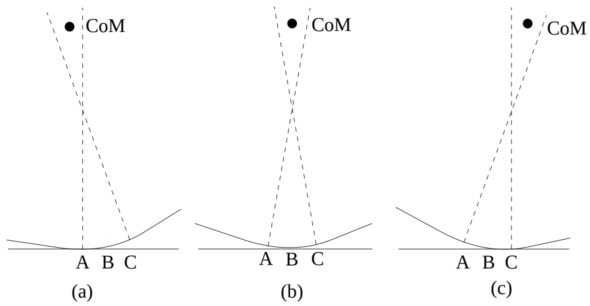

Figure 4: Perturbations about an unstable equilibrium.

object rotates clockwise towards the equilibrium contact at B in Figure 3(b). The magnitude M_γ of the cross product $\mathbf{M}_\gamma$ is negative.

In Figure 3(c) the object has been perturbed from equilibrium such that the contact point is at point C and the critical ray extends vertically up from C. The critical ray passes to the right of the CoM and thus the object rotates anti-clockwise towards the equilibrium contact at B in Figure 3(b). M_γ is positive.

Since the object returns to the equilibrium condition of Figure 3(b) for both the perturbations in Figures 3(a) and 3(c) the equilibrium point is deemed to be stable. Such an equilibrium corresponds to a point on a convergent boundary on a PSD. If we consider the sign of M_γ as we traverse the curve through contacts A, B and C it is first negative, then zero and finally positive as illustrated in Figure 5(a). The gradient of M_γ (w.r.t. arc-length) is positive for a stable equilibrium.

We can perform a similar analysis for the unstable equilibrium shown in Figure 4(b) and we see that the gradient of M_γ is negative. See Figure 5(b).

Thus, we have shown by inspection the sign of the gradient of M_γ at both stable and unstable equilibria. We will now show analytically how the curvature of an object relates to the stability of an equilibrium.

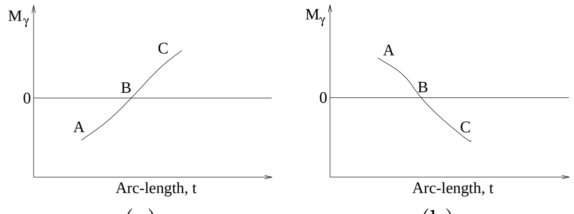

(a) The gradient of the scalar M_γ about a stable equilibrium such as that in Figure 3(b) is positive (see text). (b) The gradient of the scalar M_γ about an unstable equilibrium such as that in Figure 4(b) is negative (see text).

Figure 5: The qualitative gradient of the scalar M_γ about equilibrium points.

From Figure 2 we can see that

$$\mathbf{N}_\gamma = \cos\gamma\mathbf{N} + \sin\gamma\mathbf{T}$$

Combining this with equation (7) gives

$$\mathbf{M}_\gamma = \cos\gamma\mathbf{r}\times\mathbf{N} + \sin\gamma\mathbf{r}\times\mathbf{T}$$

Differentiating with respect to arc-length we find that the gradient of $\mathbf{M}_\gamma$ is given by

$$\mathbf{M}'_\gamma = \cos\gamma(\mathbf{r}'\times\mathbf{N} + \mathbf{r}\times\mathbf{N}') + \sin\gamma(\mathbf{r}'\times\mathbf{T} + \mathbf{r}\times\mathbf{T}')$$

Using equations (2) and (3) to (5) it follows that

$$\begin{aligned}\mathbf{M}'_\gamma &= \cos\gamma(\mathbf{T}\times\mathbf{N} - \kappa\mathbf{r}\times\mathbf{T}) + \sin\gamma(\mathbf{T}\times\mathbf{T} + \kappa\mathbf{r}\times\mathbf{N}) \\ &= \cos\gamma(\mathbf{B} - \kappa\mathbf{r}\times\mathbf{T}) + \kappa\sin\gamma\mathbf{r}\times\mathbf{N} \qquad (8)\end{aligned}$$

Now during equilibrium $\mathbf{r}$ lies along $\mathbf{N}_\gamma$ but in the opposite direction hence

$$\mathbf{r}\times\mathbf{T} = |\mathbf{r}||\mathbf{T}|\sin(\gamma + 90^o)\mathbf{B} = |\mathbf{r}|\cos\gamma\mathbf{B}$$

and

$$\mathbf{r}\times\mathbf{N} = |\mathbf{r}||\mathbf{N}|\sin(\gamma + 180^o)\mathbf{B} = -|\mathbf{r}|\sin\gamma\mathbf{B}$$

Substituting the values of these cross products into equation (8) we have

$$\begin{aligned}\mathbf{M}'_\gamma &= \cos\gamma(\mathbf{B} - \kappa|\mathbf{r}|\cos\gamma\mathbf{B}) - \sin\gamma(\kappa|\mathbf{r}|\sin\gamma\mathbf{B}) \\ &= (\cos\gamma - \kappa|\mathbf{r}|)\mathbf{B}\end{aligned}$$

Now, the direction of the derivative is $\mathbf{B}$, and the magnitude is given by

$$M'_\gamma = \cos\gamma - \kappa|\mathbf{r}|$$

So $M'_\gamma > 0$, *i.e.* an equilibrium is stable, if

$$\cos\gamma - \kappa|\mathbf{r}| > 0$$

or

$$|\mathbf{r}| < \rho\cos\gamma \qquad (9)$$

where $|\mathbf{r}|$ is the distance along the critical ray from the object's outline to the CoM. So an equilibrium orientation is stable if the distance along the critical ray to the CoM is less than the radius of curvature at the contact point multiplied by the cosine of the angle that the critical ray makes with the contact normal. Conversely, an equilibrium is unstable if the distance along the critical ray to the CoM is greater than the radius of curvature multiplied by the cosine of the critical ray angle.

For the frictionless case, where the critical ray is always along the contact point normal $\mathbf{N}$, *i.e.* $\gamma = 0$, this decision boundary is a distance ρ along each normal. This defines a curve, which is the locus of the centre of curvature, called the evolute, and can be considered to be formed by the envelope of normals [5] to the closed curve that is our object outline. In the general case, *i.e.* for an arbitrary critical ray direction, the decision boundary is a distance $\rho\cos\gamma$ from each contact point in the direction of the critical ray. The collection of all these points for each point on the object's outline form a curve which looks like a "skewed" version of the evolute and it is this curve which is the decision boundary for a critical ray of arbitrary direction, γ.

5 The Effect of Changing the Position of the CoM

In order to facilitate discussion of the above analysis Figures 6 to 9 show a series of PSD's for an ellipse where the CoM, represented by an asterisk, is progressively moved from the centre of the object in a south-easterly direction. The curved, diamond-like shape inscribed on the ellipse is the evolute. The other two inscribed shapes are the skewed evolutes formed by plotting the decision boundaries given by making inequality (9) an equation with $\gamma = \pm\theta$. The significance of these curves will be explained in the following paragraphs.

First note that the orientation of the ellipse corresponding to 0 rads is that with the pushing fence placed at the bottom-most point of its curve as it is drawn. An increase in the orientation of the ellipse corresponds to it rolling anticlockwise over the fence, so the left-most point of the ellipse corresponds to an orientation of $\frac{\pi}{2}$ rads; $\phi = \pi$ rads when the top-most point is touching the fence, and $\phi = \frac{3\pi}{2}$ rads the right-most point.

Consider initially the frictionless case, *i.e.* it is the pushing direction ray that is always the critical one. For ease of explanation assume that the pushing direction is always along the contact normal. For this scenario the ellipse has four rotational equilibria. These can be read from the PSD as the orientations where the $\delta = \frac{\pi}{2}$ rads line intersects the VTC. Their stability properties can be deduced by their relationship to the clockwise and anticlockwise reorientation regions. These four equilibria correspond to the orientations of the ellipse where a contact normal passes through the CoM. For the case shown in Figure 6, with the CoM in the centre of the ellipse, these orientations correspond to the points of highest and lowest curvature. Of these points the ones with the lowest curvature are stable because the CoM lies below the relevant part of the evolute; the points at the locations of the highest curvature are unstable because the CoM lies above the relevant part of the evolute.

From the PSD it is possible to read off the reorientation sense that will occur for any particular orientation of the ellipse w.r.t. the pushing fence. For the situation of Figure 6 we see that between the stable equilibrium A at an orientation of 0 rads and the unstable equilibrium B at an orientation of $\frac{\pi}{2}$ rads, a push (in a normal direction) anywhere along this segment of the curve results in a negative, *i.e.* clockwise, reorientation. The reorientation senses of the other curve segments between equilibria can be found similarly. We see that if we traverse the curve in the direction of increasing arc-length, if we pass from a segment that results in clockwise reorientation to a segment that results in anticlockwise reorientation the equilibrium 'passed through' is a stable one. The converse is true for an unstable equilibria.

As the CoM moves to the position shown in Figure 7(a) the rotational equilibria on the ellipse outline also move as indicated by the change in the intersection of the VTC and the $\delta = \frac{\pi}{2}$ rads line of Figure 7(b). Note how the stable and unstable equilibria C and D approach each other, both on the object perimeter and on the PSD. As the CoM crosses the evolute (Figure 8(a)) these rotational equilibria are 'annihilated' as shown by the loss of two intersections of the line $\delta = \frac{\pi}{2}$ rads with the VTC (Figure 8(b)).

It is informative to consider what this event corresponds to in terms of Mason's rule. Consider the situation shown in Figure 6. Imagine that the ellipse is being pushed at a point on its boundary that corresponds to an orientation just less than that of the unstable equilibrium D, *i.e.* just less than $\frac{3\pi}{2}$ rads. We see that the normal at this point passes to the left of the VTB so the pushing ray votes for a clockwise reorientation. The normal maintains this relationship to the VTB until the stable equilibrium at C, *i.e.* $\phi = \pi$ rads. If the object's reorienting were to cause it to overshoot this point, the normal would pass through the CoM and change its relationship w.r.t. the VTB, thus resulting in the pushing ray changing the sense of its vote (which would take the orientation back towards the stable equilibrium C).

Consider now the situation shown in Figure 7. Now if we were to start pushing the object on its boundary at a point corresponding to an orientation of just less than $\frac{3\pi}{2}$ rads we would find that it reorients anticlockwise. If, however, we start with a push between the equilibria C and D the normal again passes to the side of the VTB that votes for a clockwise reorientation. An overshoot at C would again cause the pushing ray to change its vote. The behaviour of the object under pushing is the same as before w.r.t. the equilibria.

As the CoM moves towards the evolute the equilibria C and D move closer together until as it crosses the evolute C and D 'annihilate' each other and the clockwise turning segment of the object's boundary between them 'disappears'. On the PSD this corresponds to the orientation interval between C and D (on the $\delta = \frac{\pi}{2}$ rads line) reducing and then 'disappearing'. Physically this corresponds to the situation where the pushing direction ray "loses the ability" to change its vote on the segment of the object's outline that we have been considering (*cf.* [8]). This should come as no surprise since by crossing the evolute the CoM has changed its relationship with the envelope of normals. On the PSD the pushing direction ray's inability to change its relationship w.r.t. the VTB corresponds to the VTC losing two intersections with the $\delta = \frac{\pi}{2}$ rads line. The critical point, when the pushing ray is just about to lose its ability to change its vote, is when the VTC just kisses the $\delta = \frac{\pi}{2}$ rads line, which corresponds to the CoM lying on the evolute.

A similar analysis can be conducted for the case with friction. In this situation, assuming that an object's CoM lies within its convex hull, the pushing ray never loses it ability to change its vote since it can lie anywhere on the interval $\delta =]0, \pi[$ rads. The friction cone rays however maintain a fixed relationship to the contact normal and the envelopes of these rays form the skewed evolutes. The points on an object's outline where a friction cone ray changes its vote can be found by intersecting the object's perimeter with a line tangent to the relevant section of the skewed evolute and passing through the CoM. The orientations of these points correspond to the intersections of the VTC with δ_{lfc} or δ_{rfc}. Shifting the CoM can result in the loss of a friction cone ray's ability to change its vote when the CoM is moved across the relevant skewed evolute. This is directly analogous to the effects of moving the CoM across the evolute in the frictionless case where only normal pushes are allowed (described above). An example for the ellipse is illustrated in Figure 9. The critical values where a friction cone ray is about to lose its ability to change its vote are when the VTC just kisses either δ_{lfc} or δ_{rfc}. It is these events that result in a change in the topology of the PSD due to a change in the position of the CoM.

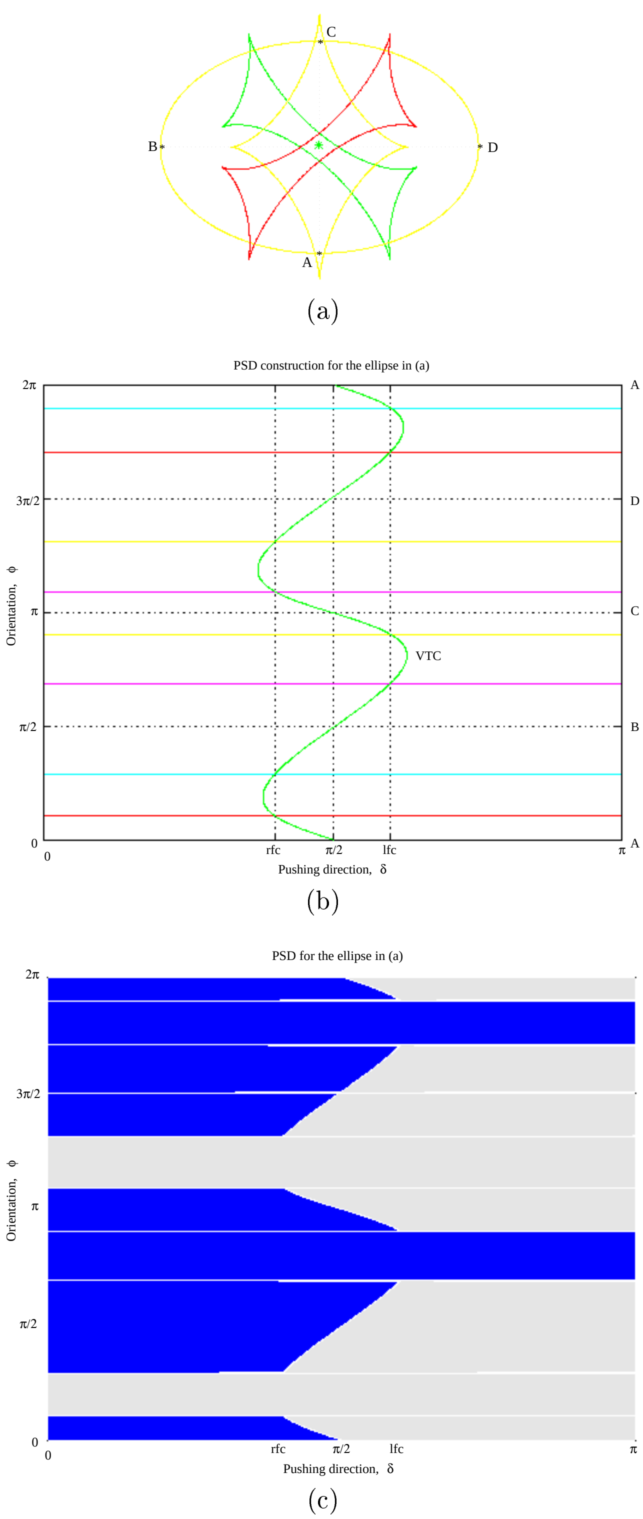

Figure 6: PSD topology with CoM inside the evolute and both friction cone skewed evolutes. Black shading denotes anticlockwise reorientation and grey clockwise.

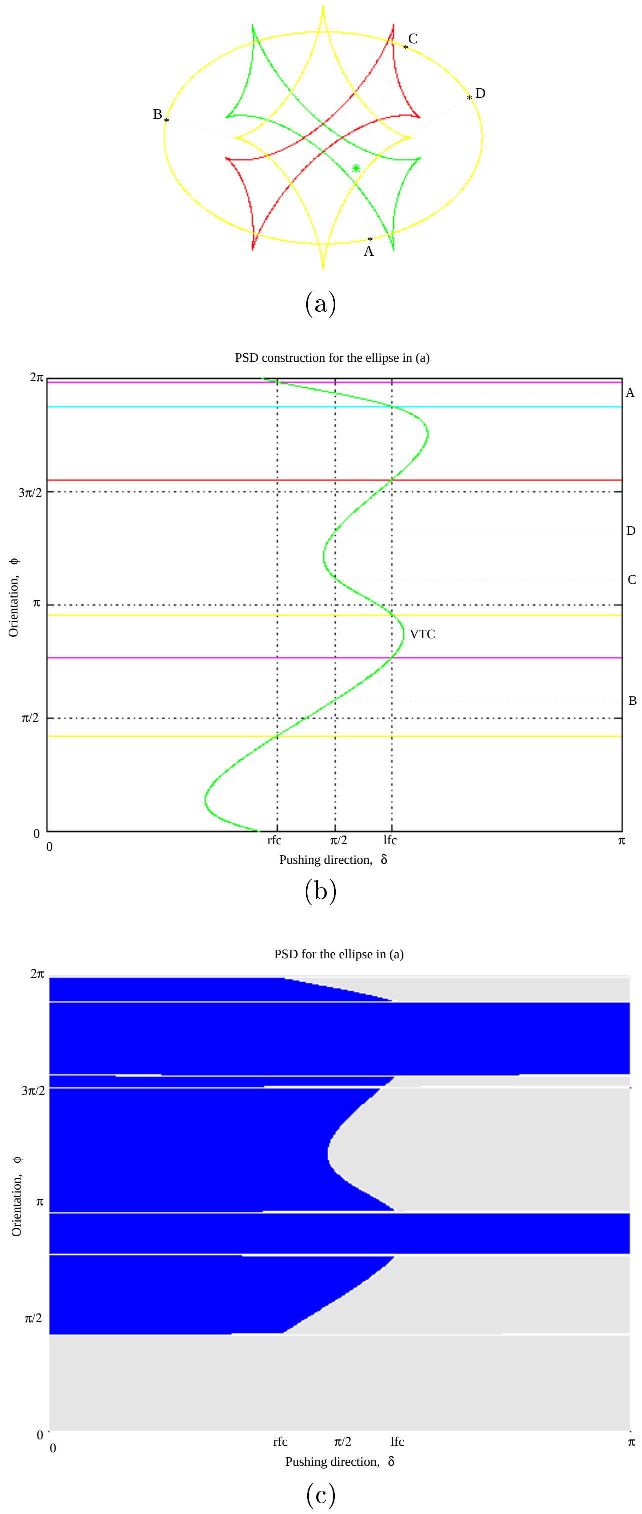

Figure 7: PSD topology with CoM inside the evolute and the left friction cone ray skewed evolute. Black shading denotes anticlockwise reorientation and grey clockwise.

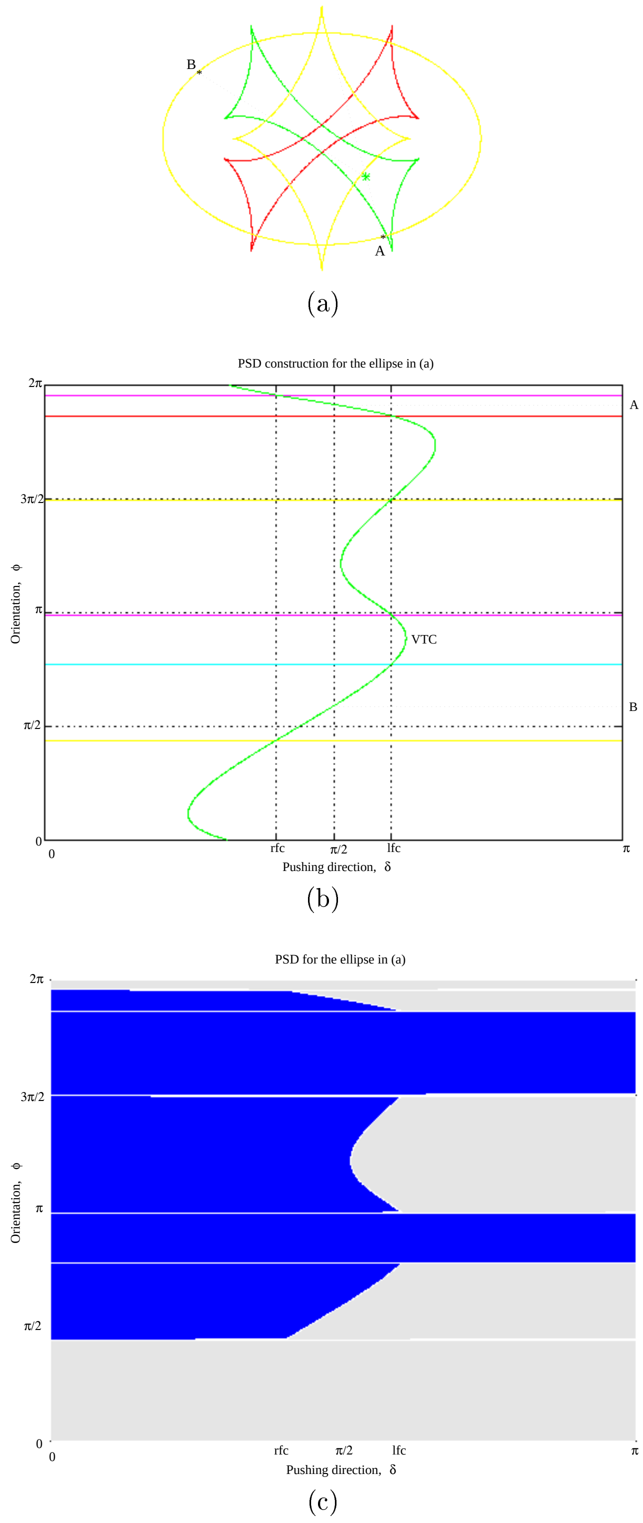

Figure 8: PSD topology with CoM outside the evolute and inside the left friction cone ray skewed evolute. Black shading denotes anticlockwise reorientation and grey clockwise.

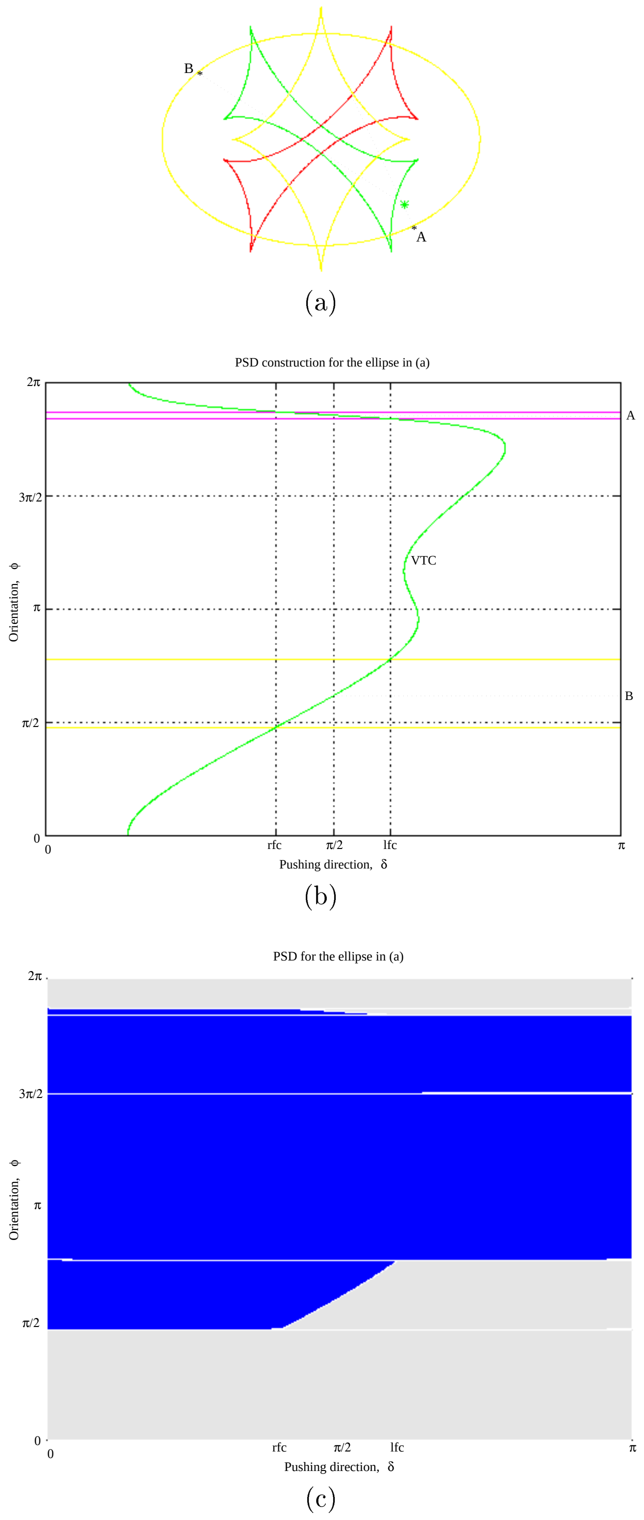

Figure 9: PSD topology with CoM outside all evolutes. Black shading denotes anticlockwise reorientation and grey clockwise.

6 Discussion

We would note here that it can be shown that the behaviour of an object being pushed under quasi-static conditions is functionally isomorphic to a gravitational catastrophe machine [17]. The analysis of the current paper and that of [8] can thus be unified as extensions to a classical catastrophe machine model. We will present this study in a further publication.

Our analysis is not limited to the pushing of parts on a horizontal surface. In [1] Akella and Mason exploit the functional equivalence between the CoM under pushing and the centre of compliance of a force-controlled robot in order to derive plans from an object's radius function [11], [9], [17], [16] to orient polygonal parts gripped by such a robot arm and pushed against a wall. The radius function correponds to the slice of a PSD where $\delta = \frac{\pi}{2}$ rads. Thus our analysis would be equally applicable to this scenario, whilst enabling extensions to objects of arbitrary shape and pushes in arbitrary directions.

7 Summary

In this paper we have investigated the conditions under which a change in the position of an object's centre of mass results in a qualitative change in its possible behaviour under pushing. We have done this by studying what the critical conditions in the vote transition curve of the Push-Stability Diagram correspond to in terms of an object's curvature. An understanding of this phenomenon gives us the ability to predict when the pushing behaviour of an object may be sensitive to the location of its centre of mass. This facilitates using the location of the centre of mass as a control parameter in a design for feeding paradigm, and provides the ability to choose robust pushing directions when orienting by pushing.

Acknowledgements

This paper was prepared whilst GED was employed on EPSRC grant GR/K 68271.

References

[1] S. Akella and M.T. Mason. Parts orienting by push-aligning. In *IEEE Int. Conf. on Robotics and Automation*, pages 414–420, Nagoya, Japan, May 1995.

[2] M. Brokowski, M. Peshkin, and K. Goldberg. Optimal curved fences for part alignment on a belt. *ASME J. of Mechanical Design*, 117:27–35, 1995.

[3] R.C. Brost. Planning robot grasping motions in the presence of uncertainty. Technical Report CMU-RI-TR-85-12, The Robotics Institute, Carnegie-Mellon University, Pittsburgh, PA, July 1985.

[4] R.C. Brost. Automatic grasp planning in the prescence of uncertainty. *Int. J. of Robotics Research*, 7(1):3–17, 1988.

[5] J.W. Bruce and P.J. Giblin. *Curves and Singularities, 2^{nd} edition.* Cambridge University Press, Cambridge, England, 1992.

[6] M. Do Carmo. *Differential Geometry of Curves and Surfaces.* Prentice-Hall, Englewood Cliffs, NJ, 1976.

[7] G.E. Deacon, P.L. Low, and C. Malcolm. Orienting objects in a minimum number of robot sweeping motions. In P.W.H. Chung, G. Lovegrove, and M. Ali, editors, *Proc. 6^{th} Int. Conf. on Industrial and Engineering Applications of Artificial Intelligence and Expert Systems*, pages 494–503, Edinburgh, Scotland, June 1993.

[8] G.E. Deacon, M. Wright, and C. Malcolm. Qualitative transitions in object reorienting behaviour, Part 1: The effects of varying friction. In *Proc. IEEE Int. Conf. on Robotics and Automation*, pages 2697–2704, Albuquerque, NM, April 1997.

[9] K.Y. Goldberg. *Stochastic Plans for Robotic Manipulation.* PhD thesis, Department of Computer Science, Carnegie-Mellon University, Pittsburgh, PA, August 1990.

[10] M. Mani and W.R.D. Wilson. A programmable orienting system for flat parts. In *Proc. North American Manufacturing Research Institute Conference XIII*, pages 427–432, Berkeley, CA, May 1985.

[11] M.T. Mason. *Manipulator Grasping and Pushing Operations.* PhD thesis, Department of Electrical Engineering and Computer Science, Massachusetts Institute of Technology, Cambridge, MA, June 1982.

[12] M.T. Mason. Mechanics and planning of manipulator pushing operations. *Int. J. of Robotics Research*, 5(3):53–71, 1986.

[13] J.L. Meriam. *Statics, 2^{nd} edition.* John Wiley and Sons, Inc., New York, NY, 1975.

[14] M.A. Peshkin. *Planning Robotic Manipulation Strategies for Sliding Objects.* PhD thesis, Department of Physics and the Robotics Institute, Carnegie-Mellon University, Pittsburgh, PA, November 1986.

[15] A.S. Rao and K.Y. Goldberg. Manipulating algebraic parts in the plane. *IEEE Transactions on Robotics and Automation*, 11(4):598–602, 1995.

[16] J. Wiegley, K. Goldberg, M. Peshkin, and M. Brokowski. A complete algorithm for designing passive fences to orient parts. In *IEEE Int. Conf. on Robotics and Automation*, pages 1133–1139, Minneapolis, MN, April 1996.

[17] M. Wright and G.E. Deacon. Orienting 2.5D objects of arbitrary shape: A computational theory of planar orientation. (Unpublished) Working Paper, Department of Artificial Intelligence, University of Edinburgh, Edinburgh, Scotland, 1996.